Scientific Justification

One lasting scientific legacy of the *Hubble Space Telescope (HST)* is the discovery of massive black holes at the centers of a substantial fraction of galaxies, confirming the longstanding theory of the "central engines" of quasars. One of the major surprises from the *Hubble* was the discovery of a strong correlation between black hole mass and host galaxy properties.[1] This connection, causal or otherwise, may provide crucial clues to how and why these black holes formed and how their host galaxies evolved. *As of the launch of the James Webb Space Telescope (JWST), the question of how black holes affect their host galaxies is one of the outstanding questions in astrophysics.*

Observational and theoretical work now suggests that active galaxies and black holes are potentially linked to both the triggering, and "quenching", of massive star formation. The link between massive galaxies and their central super-massive black holes (SMBHs) that appear ubiquitous is vital to the understanding of galaxy formation and evolution, and significant observational and theoretical effort has been invested in trying to measure and understand the physics involved in these systems.

The "quenching" of galaxy-wide star formation is supposedly driven by " AGN feedback", where the AGN heats the surrounding gas corona, offsetting cooling losses and disrupting the gas inflow. This feedback manifests itself as high-velocity outflows from the AGN. *However, strong, direct observational evidence for AGN feedback is still lacking, especially for the most luminous systems at $z = 2 - 3$, at the height of the Quasar Epoch.* We have identified the best candidates that would possess quasar feedback in action, in situ at high-redshift. These are the "Extremely Red Quasars" identified via their WISE W3/4 colors. As such, these mJy luminous AGN *are ideal targets for JWST MIRI.*

The Extremely Red Quasar Population

Extremely Red Quasars (ERQs) are a unique obscured quasar population with extreme physical conditions related to powerful outflows across the line-forming regions. These sources are the signposts of the most extreme form of quasar feedback at the peak epoch of galaxy formation, and may represent an active "blow-out" phase of quasar evolution.

By matching the quasar catalogues of the Sloan Digital Sky Survey (SDSS) and the Baryon Oscillation Spectroscopic Survey (BOSS) to the Wide-Field Infrared Survey Explorer (WISE), Ross et al. (2015) discovered quasars with extremely red infrared-to-optical colors: $r_{\rm AB} - W4_{\rm Vega} > 14$ mag, i.e., $F_\nu(22\mu{\rm m})/F_\nu(r) \gtrsim 1000$; see Figure 1. These objects have infrared luminosities $\sim 10^{47}$ erg s^{-1}, and this initial study returned a heterogeneous population, spanning a wide redshift range $0.28 < z < 4.36$.

Hamann et al. (2017) refined the selection of the ERQs, honing the definition based on additional analysis and common properties, and found more objects in this new scheme; a

[1] Assessment of Options for Extending the Life of the Hubble Space Telescope: Final Report (2005); https://www.nap.edu/read/11169/chapter/5).

core sample of 97 ERQs with nearly uniform peculiar properties selected via i–$W3 \geq 4.6$ (AB) and REW(C IV) ≥ 100 Å at redshifts 2.0–3.4. The core ERQs have median luminosity $\langle \log L(\mathrm{ergs/s}) \rangle \sim 47.1$, sky density 0.010 deg^{-2}, surprisingly flat/blue UV spectra given their red UV-to-mid-IR colors, and common outflow signatures including BALs or BAL-like features and large C IV emission-line blueshifts. They have a suite of peculiar emission-line properties including large rest equivalent widths (REWs), unusual "wingless" line profiles, large N V/Lyα, N V/C IV, Si IV/C IV and other flux ratios, and very broad and blueshifted [O III] λ5007 (e.g., Figure 1, top right). Their SEDs (Figure **??**, *left*) and line properties are inconsistent with normal quasars behind a dust reddening screen. Patchy obscuration by small dusty clouds could produce the observed UV extinctions without substantial UV reddening.

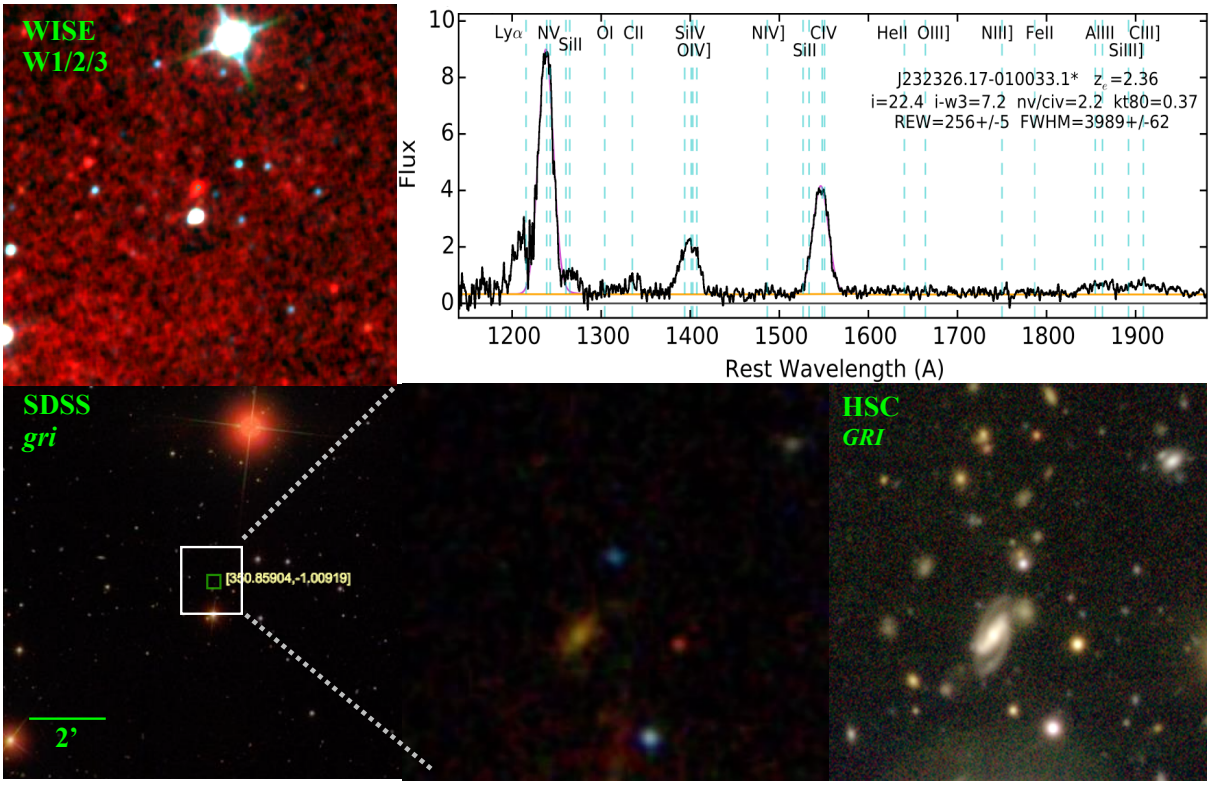

Figure 1. IR and optical imaging of J2323-0100, one of the four Extremely Red Quasar ERS targets. WISE (*top left*), SDSS (*bottom left*) with zoom-in (*bottom center*) and new HSC imaging (*bottom right*). The UV-rest frame spectrum (from Hamann et al. 2017) is given in the top right. Emission lines are labelled at positions marked by dashed blue lines. Note the unusual line flux ratios e.g., N V>Lyα and large N V /C IV. The orange and magenta curves show our fits to the continuum, and the C IV and N V emission lines, respectively. The redshift and other measured properties are also given.

Further observations by our team with VLT/XShooter measured rest-frame optical spectra of four of the $z \sim 2.5$ ERQs (Zakamska et al. 2016) which revealed very broad (FWHM = 2600-5000 km s^{-1}), strongly blue-shifted (by up to 1500 km s^{-1}) [O III] λ5007Å emission lines in these objects. In a large sample of type 2 and red quasars, [O III] kinematics are positively correlated with infrared luminosity, and the four objects in our sample are on the extreme

end both in [O III] kinematics and infrared luminosity. As such, we estimate that at least 3% of the bolometric luminosity in these objects is being converted into the kinetic power of the observed wind. Photo-ionization estimates suggest that the [O III] emission might be extended on a few kpc scales, which would suggest that the extreme outflow is affecting the entire host galaxy of the quasar.

MIR spectroscopy and PAHs: Polycyclic Aromatic Hydrocarbons (PAHs) are abundant, ubiquitous, and dominate the structure and evolution of the ISM of galaxies. Aromatic features are already a significant component of dusty galaxy spectra as early as $z \approx 2$, and the infrared (IR) emission features at 3.3, 6.2, 7.7, 8.6, and 11.3 μm are generally attributed to IR fluorescence from (mainly) far-ultraviolet (FUV) pumped large PAH molecules. *As such, these features trace the FUV stellar flux and are thus a measure of star formation.* The interstellar IR emission spectrum is incredibly rich and shows a wealth of detail. It is dominated by major PAH emission features at 3.3, 6.2, 7.7 and 8.6 μm. In addition, there are weaker features at 3.4, 3.5, 5.25, 5.75, 6.0, 6.9 and 7.5μm. *Given the redshift of our ERQs and the MIRI wavelength coverage we will cover* $1.36 \leq \lambda_{\rm emitted} \leq 8.6\mu m$. In theory, we can detect the 3μm and 6.0μm water-ice feature, and figure out *where* it is most prevalent in the quasar. Figure **??** shows an example of the current state-of-the-art in quasar MIR spectral composites with ≈60 *Spitzer* IRS quasars per bin. *We will have equivalent SNR from 1 quasar, across a broader wavelength range and in a new redshift-luminosity regime.*

The mid-IR spectral region also presents a suite of high-ionization lines: [S IX] at 1.252μm, [Si X] at 1.430μm, [Si XI] at 1.932μm, [Si VI] at 1.962μm, [Ca VIII] at 2.321μm, [Si VI] at 2.483μm [Si IX] at 3.935μm and [Ar II] at 6.97μm. However, most critically, we have access to the [Ne VI] line at 7.65μm, which with an ionization potential of 158 eV is much too high for stars. **The [Ne VI] 7.65μm line can be used to measure the instantaneous luminosity of the central engine.** [Ne VI] 7.65μm has a critical density of $\sim 10^6$ cm^{-3} and very low interstellar extinction. Its ratio to the hydrogen recombination lines is almost independent of ionization parameter thus making this a superb emission line to utilize.

With the IFU spatial information, at medium resolution, we will be able to (i) map the PAH emission structure of the extremely red quasars on sub-kiloparsec scales and (ii) look for offsets in these emissions that could well be indicative of 'AGN feedback'.

Integral Field Unit Observations: The ability for the MRS to obtain integral field unit spectroscopy allows us to investigate the *spatial information* associated with the high IR fluxes in the ERQs. The spatial distribution of the IR will give direct clues to the power source of the IR emission. The IFU aspect of the Medium Resolution Spectrometer will allow investigations in unprecedented detail of both the central AGN IR emission and any potentially extended emission in $z \approx 2.5$ quasars. As a null hypothesis, we suggest that weak PAH emission will be in the nuclear regions and strong(er) PAH emission in the extended source. However, very recent studies with Hα of $z \sim 2$ quasars suggest that narrow Hα emission might be from a spatially unresolved source.

Our final primary science goal will be to examine the IR spectral emission lines (PAH or high ionization) and place them in context with the host galaxy by looking for emission line

offsets or blends. The kinematics of the [O III] $\lambda\lambda$4959,5007 Å emission lines are *known to be extreme* in these objects, being very broad (FWHM=2600–5000 km s^{-1}) and strongly blueshifted (by up to 1500 km s^{-1}; Figure 2, *right*). We also know that the [O III] kinematics are positively correlated with infrared luminosity. Can we place the PAH and AGN emission in the same consistent kinematic structure? Is there a spatial variation of the kinematics of the IR emission lines, and if so, is it consistent with a strong 'AGN feedback' phase?

Given the pixel scales of the MRS IFU, and the fact that 1" is $\approx$*8 kpc at* $z \sim 2.5$ *a major challenge, goal and SEP will be to deliver software and analyses that samples the data on a sub-pixel scale.*

■ Technical Justification

After discussions with the MIRI Team (including European P.I., G. Wright and Instrument Scientist A. Glasse), we settled on the strategy of picking one instrument (MIRI) and one observing mode (MRS) and making sure we deliver the highest quality data analysis and SEPs in this specific instance for the community.

Due to the nature of the ERS program, we note that we do not necessarily have to observe a full, representative sample[2] *and given the Discretionary time available for the ERS, a natural program size is* $\lesssim$*35-40 hours.* Moreover, our program specifically tests only a particular mode of MIRI, albeit in detail, and thus our time request is curtailed in that manner. With these considerations in place, and with the desire to immediately gain high signal-to-noise spectra in order to investigate the physics and chemistry of quasar PAHs, along with observational overhead concerns, pushes us to observe four quasars, each object for 3.59 hours, for a total program Charged Time of 22.20 hours. The details of our four primary quasar targets are given in Table 1.
For our MIRI MRS operations we shall:

- Operate over the full spectral coverage, and thus will use all three different spectral settings; SHORT (A), MEDIUM (B), and LONG (C).
- Use the point source optimized, "4-point ALL" dither pattern. This is the only MIRI MRS dither patterns that guarantees "GOOD" (i.e. half-integer) sampling throughout the common field of view across all four channels.
- Detector Readout mode: SLOW. Our integrations are relatively long, and the 'Slow' mode readout pattern offers fewer detector artifacts and slightly lower detector noise than the 'Fast' mode, making it a good choice for faint source medium-resolution spectroscopy where the sky backgrounds are low. This is what we want for our ERQ observations.

[2]Our longer term goals will be to observe a representative sample of ERQs across a range of redshifts to access e.g., the 9.7μm silicate feature and 11.2, 12.7, and 16.4μm PAHs.

Object Name (SDSS)	J0834+0159	J1232+0912	J2215-0056	J2323-0100
Object R.A.	08:34:48.48	12:32:41.73	22:15:24.00	23:23:26.17
object declination	+01:59:21.1	+09:12:09.3	−00:56:43.8	−01:00:33.1
r-band AB magnitude	21.19±0.05	21.11± 0.05	22.27±0.12	21.62± 0.08
WISE W4-band Vega magnitude	6.88±0.09	6.78 ±0.09	7.91±0.24	7.76±0.22
WISE W4-band flux, F_ν	14.80 mJy	16.23 mJy	5.73 mJy	6.58 mJy
$i_{\rm AB} - W3_{\rm AB}$	6.0	6.8	6.2	7.2
Redshift z	2.591	2.381	2.509	2.356
REW C IV	209±6	225±3	153±5	256±5
C IV FWHM km s^{-1}	2863±65	4787±52	4280±112	3989±62
[O III] FWHM km s^{-1}	2811	4971	3057	2625
ALMA Band 6	*pending*	√	*pending*	√
HST Cycle 24 ACS+WFC3	obtained	*pending*	*pending*	*pending*
Spectro-polarimertry	×	√	√	×
Groups/Integrations/Exposures	45/1/1	15/3/1	45/1/1	15/3/1
JWST target visibility (Start)	2019-04-01	2019-05-08	2019-05-22	2019-06-07
JWST target visibility (End)	2019-05-07	2019-07-01	2019-07-15	2019-07-29

Table 1: Our four Extremely Red Quasar targets. All four quasars were first identified in Ross et al. (2015). Values of Rest Equivalent Widths (REW) and Full Width Half Maxima (FWHM) are from Zakamska et al. (2016) and Hamann et al. (2017).

We are interested in only a single object per point, so no mosaicking is necessary. The Subarray is FULL (this setting is fixed for MRS).

We desire high signal-to-noise in order to *(i)* detect any low Equivalent Width PAH or AGN emission lines that might be resolved at MRS resolutions and *(ii)* immediately compare our science results to those of the *Spitzer Space Telescope* IRS studies. *With only 4 high-SNR JWST objects, we will have similar SNR as the Spitzer IRS composite studies of* $\gg 100$ *objects, and at similar resolution.* Long integrations also minimize Observatory overhead, a desire that has been imparted on us by STScI operations.

For the observations themselves, a wide range of considerations e.g., sample size, desired high SNR, time available for ERS programs, level of read noise, novelty of instrument, utility to the SEPs, etc., went into our estimated time calculations.

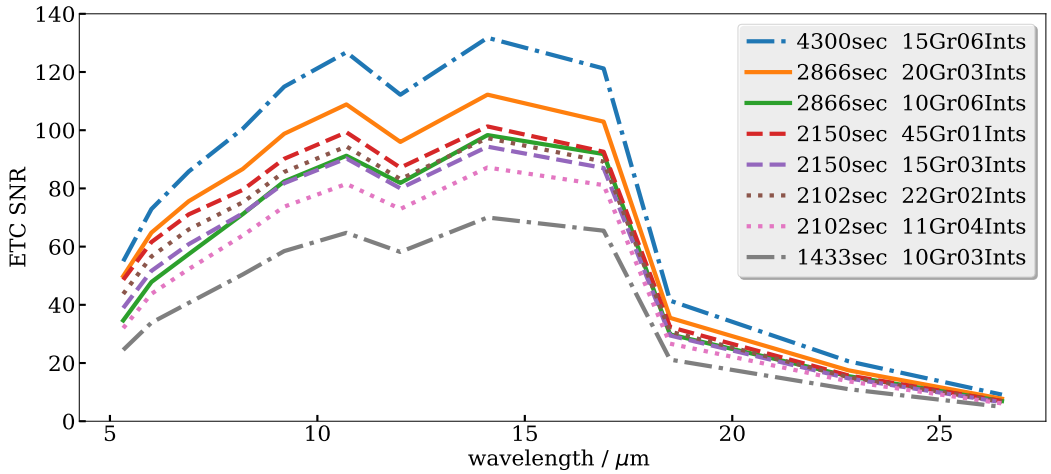

Figure 1: ETC calculations of MIRI MRS SNR values for a range of Group sizes, Integrations and the associated Science exposure time (per Wavelength disperser). The SNR is from the ETC and is per pixel. This exposure time has to be multiplied by 24 to get the full Science Exposure time: (a factor of 2 from the 2point in the ETC to 4-point dither; a factor of 3 since for all three SHORT, MEDIUM and LONG modes and a factor of 4 for the four quasars).

Our JWST ETC Workbook is `wb ID 7474`. In the ETC we assume the shape of the source is Point; a Medium Background; the 'IFU Nod In Scene'; Aperture location as centered on source; an Aperture radius of 0.3"; Nod position in scene of $X = Y = 0.5''$. We take the "core ERQ" SED that is given in Hamann et al. (2017) and is fully representative of the ERQ population at large. The file `core_ERQ_SED_notLog.dat` is used here. We normalize this SED at a wavelength of 23μm to a source flux density of 5mJy, again representative (and if anything on the fainter end) of the WISE W3/4-detected ERQ population and our targets. At this stage we *do not* include any emission (or absorption) lines since our null hypothesis we want to test is that the IR emission is purely from an AGN power-law.

Figure 1 shows our resulting SNR values for a range of Group, Integrations and Exposures. We ultimately decided to go with two combinations of the Groups/Integrations/Exposures, for the same total Science Exposure time; see Table 1. Our final observing time request is 3.59 hours Science exposure hours per object for 14.35 Science hours total. *Using Smart Accounting, the total Charged Time is 22.20 hours.*

Object name, SDSS J	R.A. (J2000)	Decl (J2000)
J000610.67+121501.2	00:06:10.6778	+12:15:01.274
J014111.13-031852.5	01:41:11.1369	-03:18:52.567
J083200.20+161500.3	08:32:00.2000	+16:15:00.300
J113721.46+142728.8	11:37:21.4663	+14:27:28.879
J121704.70+023417.1	12:17:04.7013	+02:34:17.151
J134254.45+093059.3	13:42:54.4591	+09:30:59.396
J135608.32+073017.2	13:56:08.3200	+07:30:17.200
J162518.66+144509.9	16:25:18.6600	+14:45:09.900
J215855.10-014717.9	21:58:55.1028	-01:47:17.973
J222307.12+085701.7	22:23:07.1253	+08:57:01.735

Table 2: A list of Secondary targets. All of these objects will have ALMA Cycle 5 Band 6 observations. Observations of these would allow us to achieve our SEP and Science goals.

Special Requirements (if any)

Justify Coordinated Parallel Observations (if any)

Justify Duplications (if any)

Data Processing & Analysis Plan (AR only)

Management Plan (AR only)